Appendix Figures and Tables

For the manuscript

Structure and mechanism of a eukaryotic ceramide synthase complex

Tian Xie, Qi Fang, Zike Zhang, Yanfei Wang, Feitong Dong, and Xin Gong*

*To whom correspondence should be addressed: X.G. (gongx@sustech.edu.cn).

Table of contents

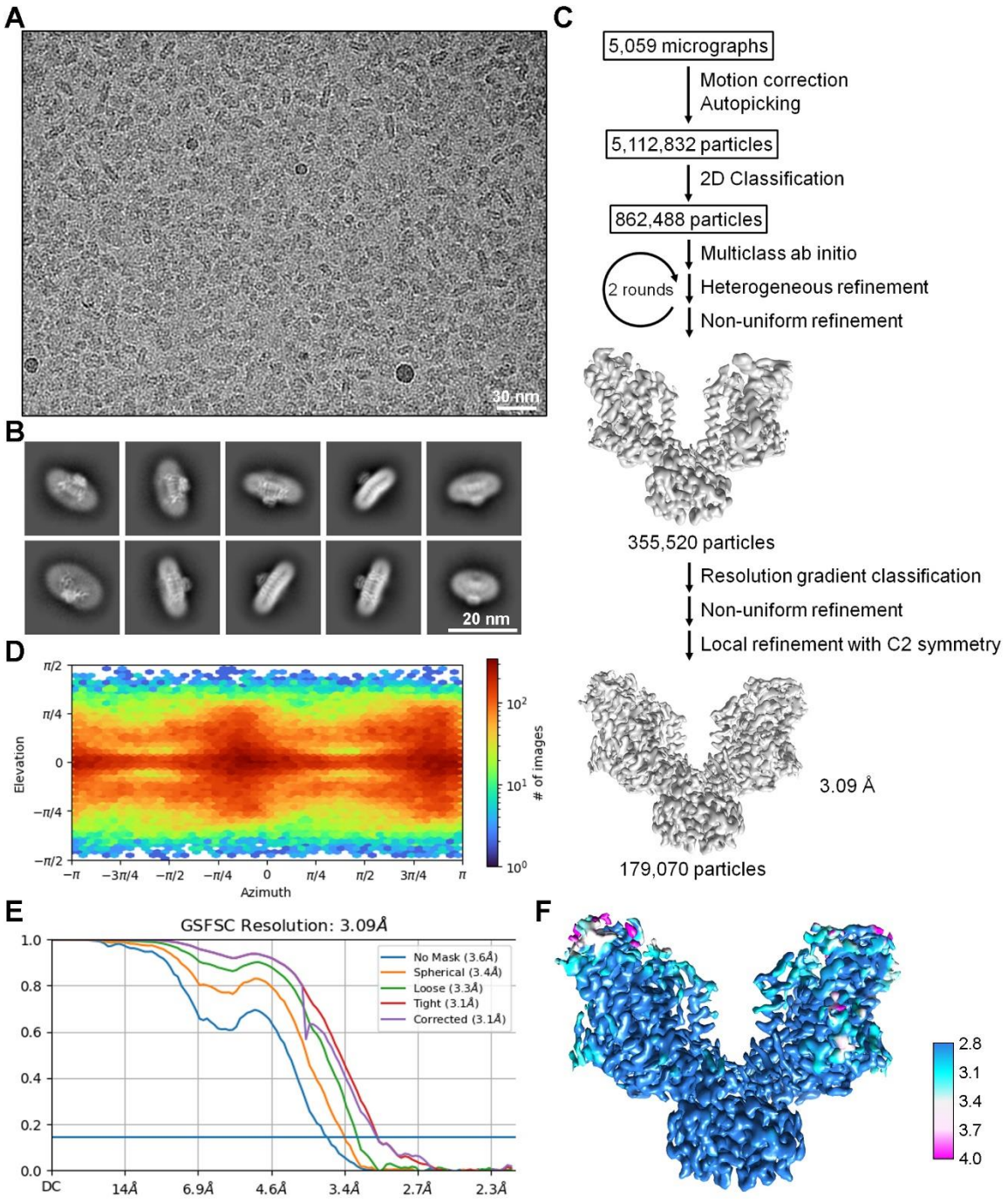

Appendix Figure S1 | Cryo-EM analysis of the C26-CoA-bound Lac1-Lip1 complex. **A,** Representative cryo-EM micrograph. **B,** Representative 2D class averages. **C,** Flowchart for cryo-EM data processing. **D-F,** Euler angle distribution, gold-standard FSC curves, and local resolution map of the C26-CoA-bound Lac1-Lip1 complex.

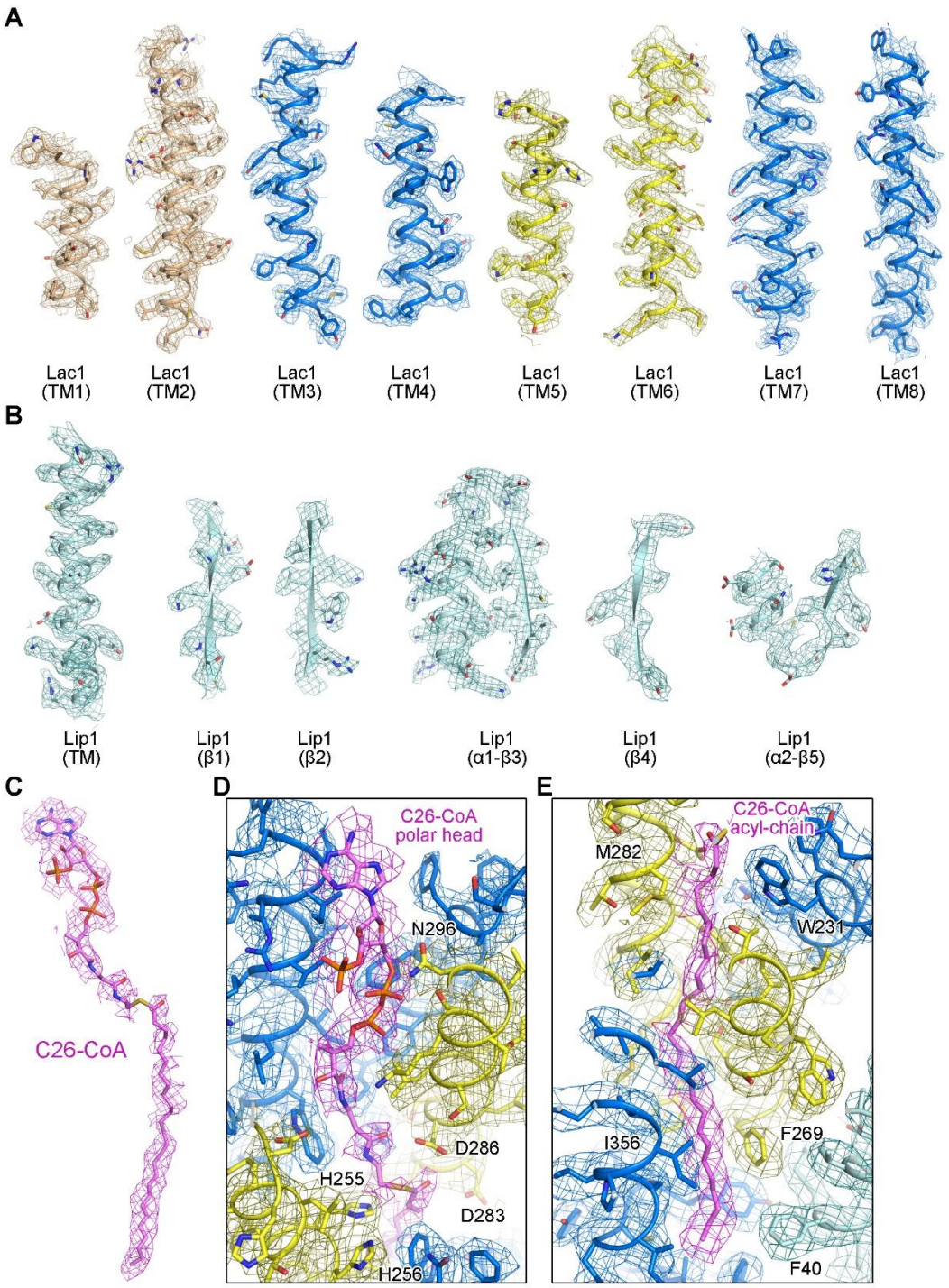

Appendix Figure S2 | Representative density maps of the C26-CoA-bound Lac1-Lip1 complex. **A-B,** EM density maps of the representative secondary structural elements from Lac1 (**A**) and Lip1 (**B**). **C,** Density map for C26-CoA. **D-E,** Close-up views of the density map for C26-CoA-binding sites. The density maps for C26-CoA were contoured at 3σ. All the other density maps were contoured at 5σ.

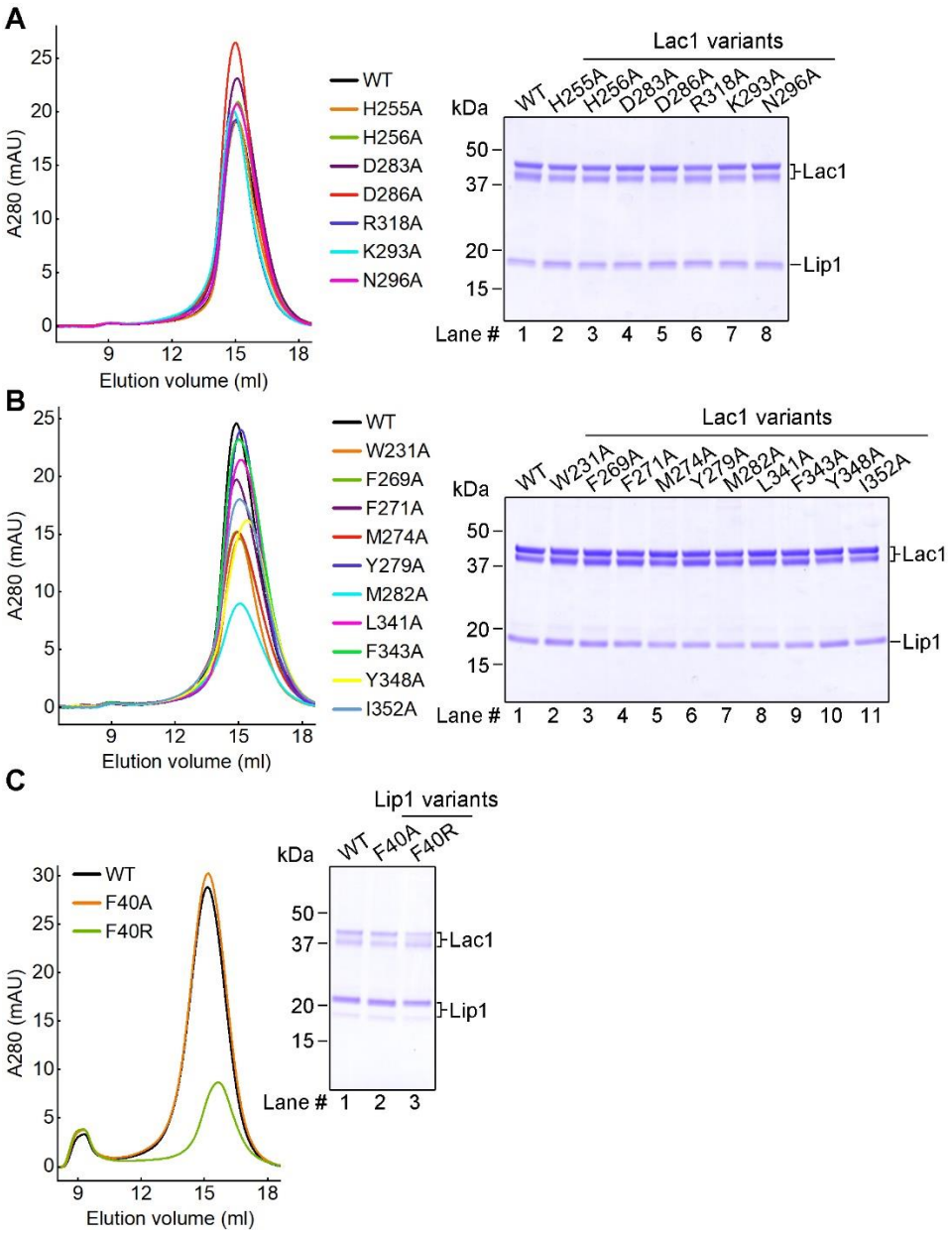

Appendix Figure S3 | Purification of C26-CoA binding mutants. SEC profiles and Coomassie blue-stained SDS-PAGE gels for the Lac1 hydrophilic cavity mutants (**A**), the Lac1 acyl-chain binding site mutants (**B**), and the Lip1 acyl-chain binding site mutants (**C**). Similar amounts of purified proteins were subjected to SDS-PAGE gels for analysis.

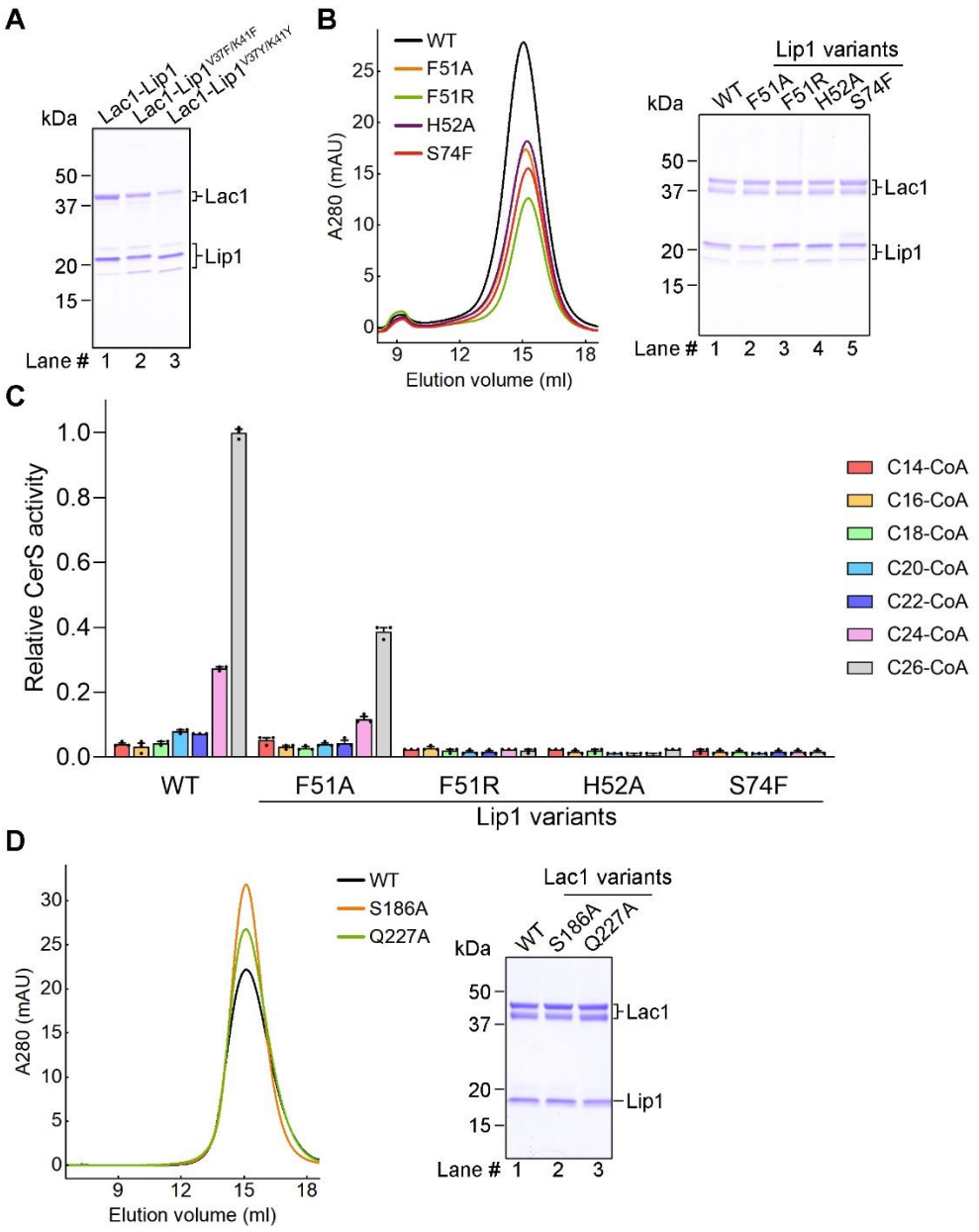

Appendix Figure S4 | Characterization of Lac1-Lip1 mutants. **A,** The Lip1 TM interaction interface mutants partially impaired the complex formation between Lac1 and Lip1. **B,** SEC profiles and Coomassie blue-stained SDS-PAGE gel for the Lip1 luminal interaction interface mutants. **C,** Acyl-chain selectivity of the Lip1 luminal interaction interface mutants revealed by CerS activity. Each data point is the average ± SEM of three independent experiments. **D,** SEC profiles and Coomassie blue-stained SDS-PAGE gel for the Lac1 lateral-opening mutants. Similar amounts of purified proteins were subjected to SDS-PAGE gels for analysis in panels (**B**) and (**D**).

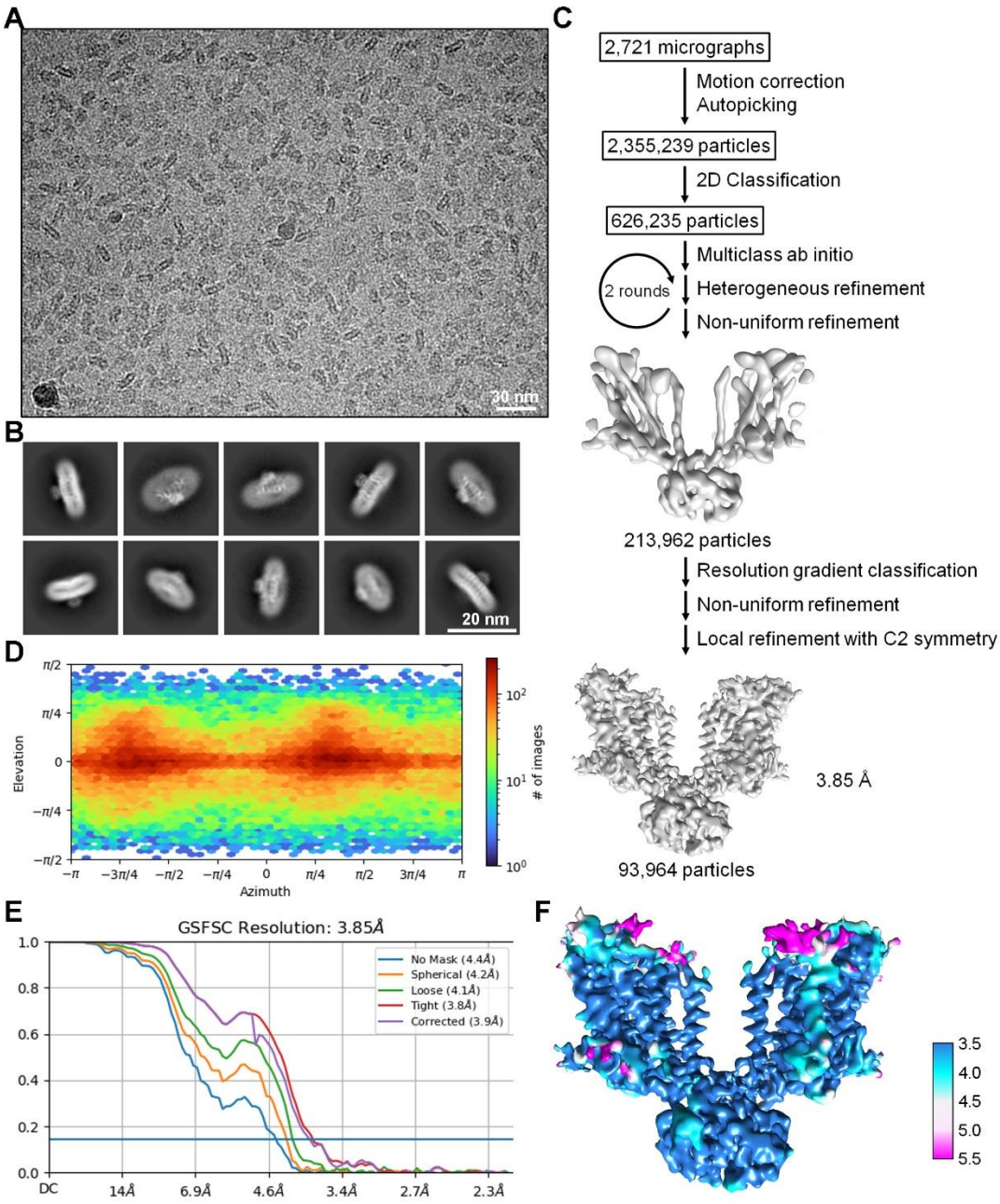

Appendix Figure S5 | Cryo-EM analysis of the Lac1-Lip1^{S74F} complex. **A,** Representative cryo-EM micrograph. **B,** Representative 2D class averages. **C,** Flowchart for cryo-EM data processing. **D-F,** Euler angle distribution, gold-standard FSC curves, and local resolution map of the Lac1-Lip1^{S74F} complex.

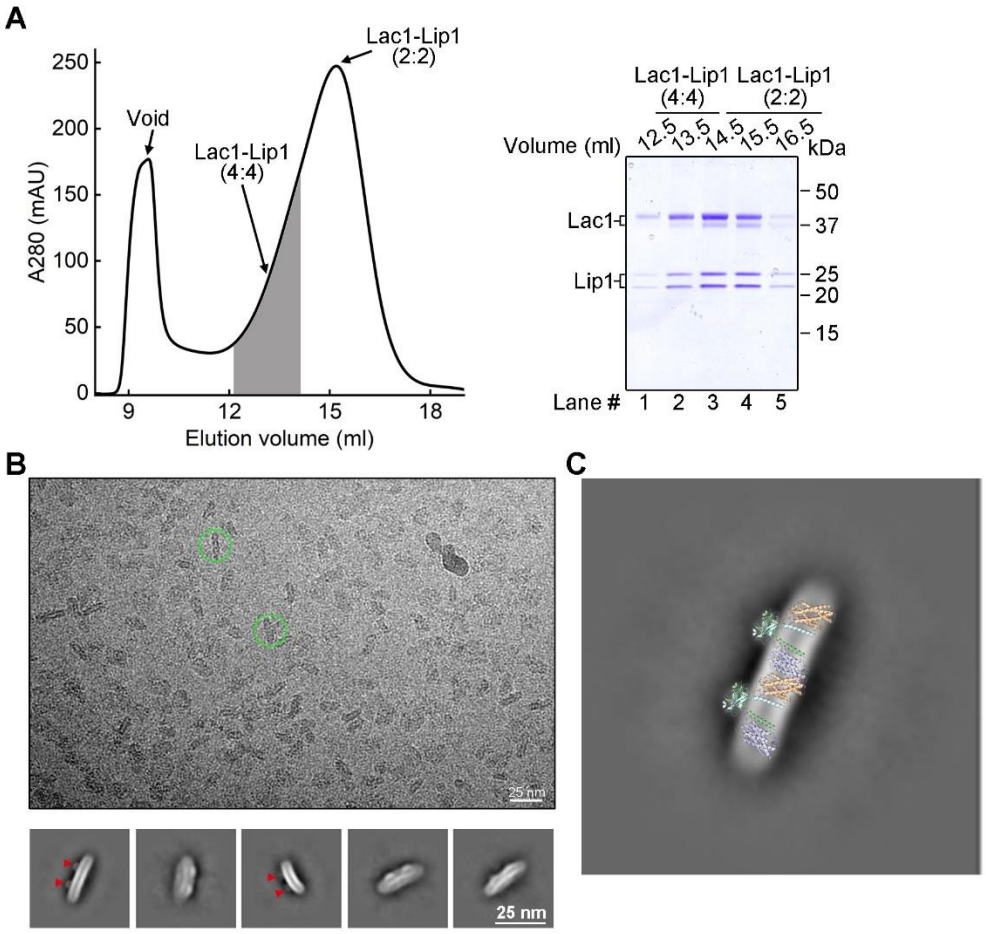

Appendix Figure S6 | Lac1-mediated oligomerization of the Lac1-Lip1 complex. **A,** SEC profile of a representative large-scale Lac1-Lip1 complex preparation. The major peak indicates the Lac1-Lip1 (2:2) complex as verified by cryo-EM analysis in Appendix Figure S1. Protein in the shoulder area before the Lac1-Lip1 (2:2) peak was collected for cryo-EM study and verified as Lac1-Lip1 (4:4) complex. **B,** Representative cryo-EM micrograph and 2D averages of the protein sample from the shoulder area. The typical Lac1-Lip1 (4:4) complex particles are indicated by green circles. The two Lip1 dimers are marked with red arrowheads. **C,** The representative 2D class average of the protein sample from the shoulder area can match well with the structures of two 2:2 Lac1-Lip1 complexes, revealing a potential Lac1-mediated oligomerization interface.

Appendix Table S1 | Cryo-EM data collection, refinement, and validation statistics.

	C26-CoA-bound Lac1-Lip1 complex (EMD-35862, PDB 8IZD)	Lac1-Lip1^{S74F} complex (EMD-35863, PDB 8IZF)
Data collection and processing		
Magnification	81,000	81,000
Voltage (kV)	300	300
Electron exposure (e^{-}/Å^2)	50	50
Defocus range (μm)	-2.0 to -1.0	-2.0 to -1.0
Pixel size (Å)	1.072	1.072
Symmetry imposed	C2	C2
Initial particle images (no.)	5,112,832	2,355,239
Final particle images (no.)	179,070	93,964
Map resolution (Å)	3.09 Å	3.85 Å
FSC threshold	0.143	0.143
Map resolution range (Å)	2.8-4.0 Å	3.5-5.5 Å
Refinement		
Initial model used (PDB code)	None	None
Model resolution (Å)	3.1 Å	3.9 Å
FSC threshold	0.143	0.143
Model resolution range (Å)		
Map sharpening *B* factor (Å^2)	-117.8	-162.5
Model composition		
Nonhydrogen atoms	7,782	7,594
Protein residues	894	894
Ligands	8	2
B factors (Å^2)		
Protein	52.04	76.45
Ligand	52.21	69.24
R.m.s. deviations		
Bond lengths (Å)	0.005	0.005
Bond angles (°)	1.224	0.891
Validation		
MolProbity score	2.02	2.23
Clashscore	11.29	15.54
Poor rotamers (%)	0.00	0.00
Ramachandran plot		
Favored (%)	93.00	90.52
Allowed (%)	7.00	9.03
Disallowed (%)	0.00	0.45